STUDIA UBB CHEMIA, LXX, 1, 2025 (p. 101-110)
(RECOMMENDED CITATION)
DOI:10.24193/subbchem.2025.1.07

DEDICATED TO THE MEMORY OF Professor RODICA MICU-SEMENIUC, whose contributions to science and education within the Faculty of Chemistry and Chemical Engineering of Babeş-Bolyai University were longstanding and far-reaching. She was, and still continues to be, an inspiration for all of us.

THE MOLECULAR AND SUPRAMOLECULAR STRUCTURE OF Mn(4,4'-DIAMINOBIPHENYL)$_2$(NCS)$_2$(EtOH)$_2$

Radu F. SEMENIUC[a,*], **Tiffany M. Smith PELLIZZERI**[a]

ABSTRACT. The title compound was prepared from $MnCl_2 \cdot 4 H_2O$ in the presence of KSCN and 4,4'-diaminobiphenyl (DABPh), using ethanol as a solvent. The complex was thoroughly characterized by elemental analysis, IR spectroscopy, and single crystal X-ray diffraction. The coordination mode of the SCN^- anion (*i.e.* Mn – NCS *vs.* Mn – SCN) was investigated, and it was found that in the solid state the manganese(II) ion is coordinated by two SCN^- ligands N-bonded to the metallic center. The coordination sphere around the metal also contains two DABPh and two ethanol molecules. The supramolecular structure of the complex is held together by several O – H ··· N and N – H ··· S hydrogen bonds. These interactions build up a 3D grid with the Mn atoms positioned in the corners of an 8.548 Å x 13.809 Å x 14.622 Å parallelepiped.

Keywords: *Manganese(II), 4,4'-diaminobiphenyl, isothiocyanate, single crystal X-ray diffraction structure, hydrogen bonds, supramolecular structure.*

INTRODUCTION

Among ambidentate ligands like the cyanide, cyanate, nitrite, nitrosobenzene, 4,4'-bipyrimidine, and nicotinate species, the thiocyanate ion is one of the most studied [1]. Considering the coordination patterns of the $[NCS]^-$

---

[a] *Department of Chemistry and Biochemistry Eastern Illinois University, 600 Lincoln Ave, Charleston, IL 61920, USA*
[*] *Corresponding author: rsemeniuc@eiu.edu*

anion, hard metals tend to form N-bonded complexes (isothiocyanates), while soft metal ions prefer the S-coordination mode (thiocyanates). Illustrating these different bonding modes, $K_2[Co(NCS)_4]$ H_2O 2 CH_3NO_2 [2], $[Mn(py)_4(NCS)_2]$ [3], $Ba[Co(NCS)_4]$ 7 H_2O [4], and $Ni(NCS)_2(Py)_4$ [5] are typical examples for N-coordination, while the octahedral $(Ph_4P)_3[Rh(SCN)_6]$ [6] and $(Me_4N)_3[Ir(SCN)_6]$ [7], square planar $(n\text{-}Bu_4N)_2[M(SCN)_4]$ (M = Pd, Pt [8]), and tetrahedral $K_2[Hg(SCN)_4]$ [9] illustrate the S-coordination of the NCS^- moiety to the metallic center. On another hand, the structures of $(n\text{-}Bu_4N)_2[Re(NCS)_6]$ [10] and $[Ph_2P(n\text{-}Pr)NMe_2]Pd[(NCS)(SCN)]$ [11] feature linkage isomerism, where both the SCN^- and NCS^- coordination modes were encountered.

The IR spectra of these species can provide some insight into the coordination mode of the anion to the metallic center. This can be investigated by identifying the position of the C–N stretching vibration, where a band about 2060 cm^{-1} indicates an N-coordination (M-NCS), while a band around 2100 cm^{-1} and above suggests an S-coordination (M-SCN) of the ligand to the metal center [12-14]. However, it has been suggested that the coordination mode of the SCN^- ligand to the metal might be influenced by the anion concentration in solution [14].

In the early 1970's, Macarovici and Micu-Semeniuc studied metal complexes of the type $[MnL_2(NCX)_2]$, $[MnL1(NCX)_2]$, $[Mn(L2)_3(NCX)_2]$, and $[Mn(L3)_3(NCX)_2]$ (X = S, Se; L, L1, and L2 = 2,2'-, 3,3'-, and 4,4-diamino-biphenyl, respectively, and L3 = bis(p-aminophenyl)methane) [15]. The complexes were characterized by IR, reflection spectra and magnetic susceptibility, and based on those studies, it was proposed that all complexes were six-coordinated. Regarding their structures, it was suggested that the compounds based on the 2,2'- and 4,4'-diaminobiphenyl ligands were discrete species, while those incorporating the 3,3'-derivative were polymeric. In this work, we revisit the synthesis and characterization of the manganese(II) complex bearing two 4,4'-diaminobiphenyl (4,4'-DABPh), two SCN^-, and two EtOH ligands, in an attempt to definitely establish the coordination mode of the SCN^- group to the metal. In addition, given the bridging nature of the 4,4'-DABPh ligand, we also wanted to determine if the compound is a discrete species or a coordination polymer.

RESULTS AND DISCUSSION

The reaction of 4 4'-diaminobiphenyl, manganese(II) chloride and potassium thiocyanate in ethanol yielded the corresponding metal complex $Mn(4,4'\text{-}DABPh)_2(NCS)_2(EtOH)_2$ as a light, air, and moisture stable species, as pictured in Scheme 1.

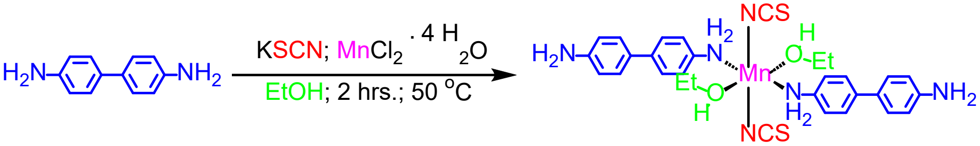

Scheme 1. Synthesis of Mn(4,4'-DABPh)$_2$(NCS)$_2$(EtOH)$_2$.

The complex is soluble in various organic solvents, but not in diethyl ether and hexanes. Its composition and structure have been established based on its analytical, spectral, and single-crystal X-ray diffraction data. Analytical data showed a metal to ligands ratio of 1 : 2 : 2 : 2. The IR spectrum of the complex recorded in a KBr matrix is typical for these types of compounds, with no unusual features. Of note however, are the characteristic CN and CS stretching and NCS bending vibrations of the SCN^- group, appearing at 2065, 821, and 478 cm^{-1}, respectively. This data implies that the Mn(II) ion is coordinated by the SCN^- group through its N atom.

Definite proof of the structure of the metal complex, and especially of the coordination mode of the SCN^- moiety, came from X-ray crystallographic studies. Relevant crystal data and structure refinement details are provided in the experimental section. Selected bond lengths and bond angles are given in Table 1 and the structure is pictured in Figure 1. The molecule consists of one manganese(II) cation coordinated by two 4,4'-DABPh and two EtOH ligands. The neutrality of the complex is ensured by the two N-bonded SCN^- anions. The bond lengths and bond angles fall within the normal range found for these types of compounds.

Table 1. Selected bond lengths [Å] and angles [°] for Mn(4,4'-DABPh)$_2$(NCS)$_2$(EtOH)$_2$.

Mn1-O1	2.165(2)	N1-C1	1.154(4)
Mn1-N1	2.173(3)	S1-C1	1.646(4)
Mn1-N2	2.294(3)	O1-H1	0.844(19)
N2-H2A	0.964(19)	N2-H2B	0.967(18)
O1-Mn1-O1#1	180.00(13)	N1-Mn1-N1#1	180.0
N2-Mn1-N2#1	180.00(12)	N1-Mn1-N2	89.74(11)
N1#1-Mn1-N2	90.26(11)	N1#1-Mn1-N2#1	89.74(11)
O1-Mn1-N1	88.52(10)	O1-Mn1-N2	91.45(9)
O1-Mn1-N1#1	91.48(10)	O1#1-Mn1-N1#1	88.52(10)
O1#1-Mn1-N1	91.48(10)	O1#1-Mn1-N2	88.55(9)
O1-Mn1-N2#1	88.55(9)	O1#1-Mn1-N2#1	91.45(9)
N1-Mn1-N2#1	90.26(11)	N1-C1-S1	179.2(3)

Symmetry transformations used to generate equivalent atoms:
#1: -x+1, -y+1, -z+1

All ligands are positioned in a *trans* orientation around the Mn^{2+} ion, with an overall D_{4h} geometry of the MnN_4O_2 skeleton. The Mn1-O1, Mn1-N1, and Mn1-N2 bond lengths are 2.165(2) Å, 2.173(3) Å, and 2.294(3) Å, and the N1-Mn1-N2, O1#1-Mn1-N1, and O1-Mn1-N2#1 angles are 89.74(11)°, 91.48(10)°, and 88.55(9)°, respectively. Given these values, the geometry around the manganese(II) center can be described as a slightly distorted octahedron.

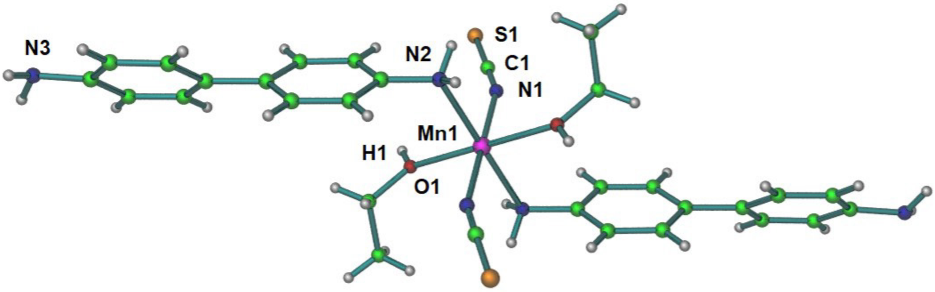

Figure 1. The molecular structure of the $Mn(4,4'\text{-}DABPh)_2(NCS)_2(EtOH)_2$ complex.

The (S)C-N-M angle is another geometrical parameter of interest. Coordination of the ligand through either the nitrogen or sulfur atoms occurs at various bonding angles [16]. In the case of isothiocyanates, the (S)C-N-M angle is closer to 180°, whereas for thiocyanates, the (N)C-S-M angle is usually found to be around 100°. These differences between the C-N-M and C-S-M bonding angles were observed for both terminal and bridging groups. In the case of $Mn(4,4'\text{-}DABPh)_2(NCS)_2(EtOH)_2$, the C-N-M angle was found to be 158.1(3)°, as observed with other compounds where the SCN^- species acted as a N-bonded ligand.

The supramolecular structure of the complex consists of chain-like architectures, held together by O – H ··· N and N – H ··· S hydrogen bonds [17], as shown in Figure 2. The ethanolic -OH functional group is involved in a close contact with the N3 atom positioned on a neighboring molecule, as seen in Figure 2a. On another hand, there are several N – H ··· S contacts involving the amine groups on the 4,4'-DABPh donor set and the S atom of the SCN^- anion, as depicted in Figure 2b-e. The geometrical parameters for these interactions are listed in Table 2. These distances are well below the sum of the van der Waals radii for hydrogen and nitrogen or hydrogen and sulfur, and the donor – hydrogen – acceptor angles are all above 140°, a clear indication of the formation of these hydrogen bonds [18].

Table 2. Geometrical parameters associated with the O – H ··· N and N – H ··· S hydrogen bonds.

Atoms	H ··· A distance (Å)	D ··· A distance (Å)	D – H – A angle (°)
O1 – H1 ··· N3	1.970	2.805	169.94
N2 – H2A ··· S1	2.521	3.392	150.35
N2 – H2B ··· S1	2.581	3.522	165.49
N3 – H4A ··· S1	2.512	3.403	169.41
N3 – H4B ··· S1	2.794	3.572	147.58

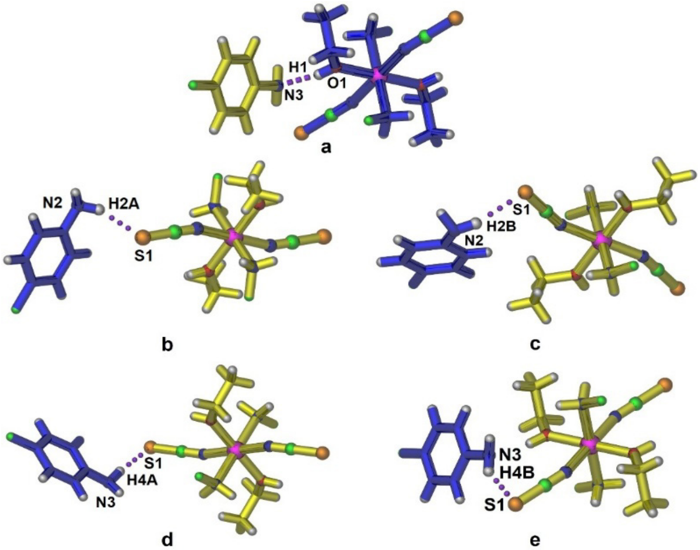

Figure 2. Details of the a) O – H ··· N and b-e) N – H ··· S hydrogen bonds in Mn(4,4'-DABPh)$_2$(NCS)$_2$(EtOH)$_2$.

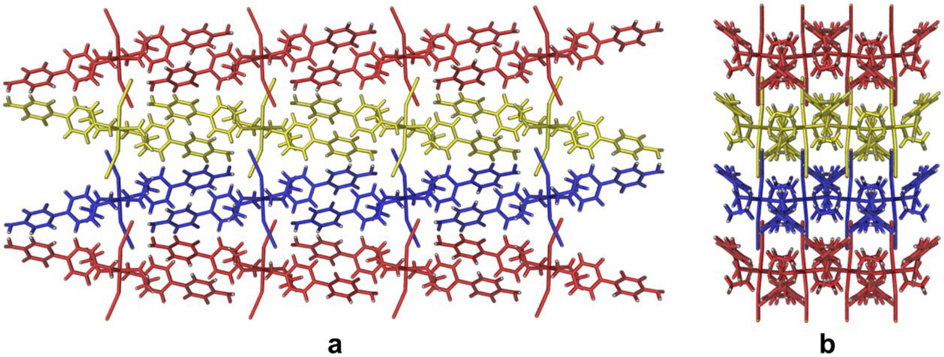

Figure 3. The crystal packing of the Mn(4,4'-DABPh)$_2$(NCS)$_2$(EtOH)$_2$ complex: a) along the *b* axis of the unit cell; b) along the *c* axis of the unit cell.

The O – H ··· N interactions build up 1D chains along the *c* axis of the unit cell, and the N – H ··· S contacts extend the supramolecular structure into a 3D array along the *b* axis of the unit cell, as pictured in Figure 3. Within this framework, the manganese(II) ions are positioned at 13.81 Å, 8.12 Å, and 14.62 Å apart, thus generating a grid-like array of the metallic centers, as seen in Figure 4.

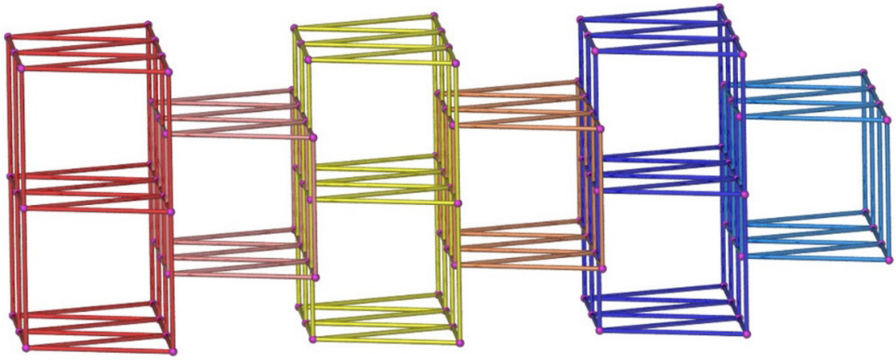

Figure 4. The grid-like arrangement of the manganese(II) cations in the $Mn(4,4'\text{-}DABPh)_2(NCS)_2(EtOH)_2$ complex.

Comparing the structure described here with similar ones found in the literature, such as bis(4,4'-diaminodiphenylmethane)-diaqua-dichloro-Mn(II) [19] (see Figure 5) it can be seen that there are obvious structural differences between their molecular structures, with the latter complex having an overall D_{2h} geometry of the $MnN_2O_2Cl_2$ skeleton. However, there are some interesting similarities between their supramolecular structures, originating from the O – H ··· Cl and N – H ··· Cl hydrogen bonds, pictured in Figure 5 as dotted and dashed lines. In both compounds the building blocks are organized by these non-covalent interactions into three-dimensional architectures. The geometrical parameters associated with these interactions in bis(4,4'-diaminodiphenylmethane)-diaqua-dichloro-Mn(II) are listed in Table 3.

Table 3. Geometrical parameters associated with the O – H ··· Cl and N – H ··· Cl hydrogen bonds.

Atoms	H ··· A distance (Å)	D ··· A distance (Å)	D – H – A angle (°)
O1w – H1w2 ··· Cl	2.164	3.116	165.22
N1 – H1B ··· Cl	2.880	3.654	144.97

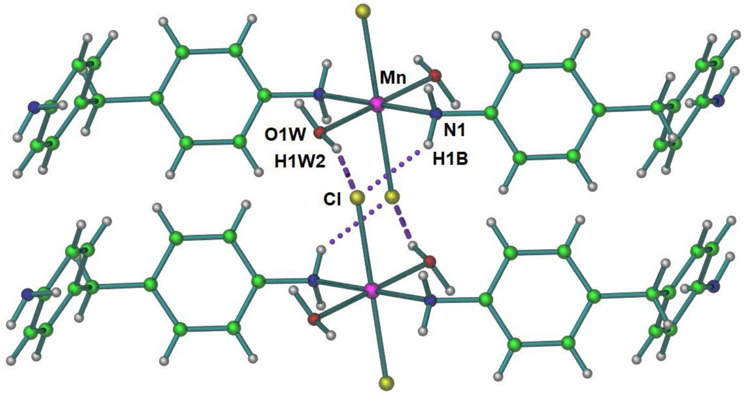

Figure 5. The structure of bis(4,4'-diaminodiphenylmethane)-diaqua-dichloro-Mn(II), and details of the O – H ··· Cl and N – H ··· Cl hydrogen bonds.

CONCLUSIONS

The reaction of 4 4'-DABPh, Mn(II) chloride and KSCN produced the Mn(4,4'-DABPh)$_2$(NCS)$_2$(EtOH)$_2$ complex. The characteristic CN and CS stretching and NCS bending vibrations of the SCN$^-$ group, were identified at 2065, 821, and 478 cm^{-1}, respectively. Structural studies showed that the molecule consists of one manganese(II) cation coordinated by two 4,4'-DABPh, two N-bonded SCN$^-$ anions, and two EtOH ligands. All these ligands are positioned in a *trans* orientation around the Mn^{2+} ion, with an overall D_{4h} geometry of the MnN_4O_2 skeleton. The Mn(4,4'-DABPh)$_2$(NCS)$_2$(EtOH)$_2$ molecules are associated into a three-dimensional grid-like supramolecular array by O – H ··· N and N – H ··· S hydrogen bonds.

EXPERIMENTAL SECTION

General information. All operations were performed in an ambient atmosphere. Infrared spectroscopy was performed on a Nicolet iS10 in a KBr matrix. All the reagents and solvents used in the synthesis described below are commercially available (Sigma-Aldrich and Oakwood) and used without further purification. Thiocyanate salts are harmful if swallowed or inhaled and can cause irritation to skin, eyes, and respiratory tract.

Synthesis of Mn(4,4'-DABPh)$_2$(NCS)$_2$(EtOH)$_2$. A 100 mL flask was charged with a stirring bar, 4 4'-diaminobiphenyl (0.184 g, 1 mmol) and 50 mL ethanol. To this solution was added $MnCl_2 \cdot 4\ H_2O$ (0.099 g, 0.5 mmol) and KSCN (0.097 g, 1 mmol). The clear solution was stirred for two hours at 50° C. The solution was then filtered to remove any solid impurities, transferred into a 100 mL beaker and loosely covered with aluminum foil. Over three days, slow evaporation of this solution afforded the title compound as single crystals. Yield of the crystalline material 0.137 g (43.4 %). If desired, more material can be isolated by completely removing the solvent. The crystalline material obtained as described above was used in all subsequent experiments. Anal. Calcd. (%) for $C_{30}H_{36}MnN_6O_2S_2$: C, 57.04; H, 5.74; N, 13.30; found C, 57.34; H, 5.44; N, 13.68; selected IR (KBr matrix, cm^{-1}): CN stretch 2065 (s), CS stretch 821 (m), NCS bend 478 (w).

Crystallographic studies. A specimen of Mn(4,4'-DABPh)$_2$(NCS)$_2$(EtOH)$_2$ ($C_{30}H_{36}MnN_6O_2S_2$, 0.240 mm x 0.350 mm x 0.420 mm) was used for the X-ray crystallographic analysis. The X-ray intensity data were measured using a Bruker Smart Apex 2 diffractometer with CuKα radiation (λ = 1.54178 Å) and a temperature of 100K. The Apex 3 software suite was used for data collection, data processing (SAINT), scaling, and absorption correction (SADABS, multi-scan) [20]. The space group of the structure was determined using XPREP, the structure solution was found by using the intrinsic phasing method (SHELXT), and the structure was refined by full-matrix least-squares methods on F^2 (SHELXL), which are all a part of the Bruker SHELXTL Software Package [21]. All non-hydrogen atoms were refined anisotropically, while hydrogen atoms were placed in calculated positions using appropriate riding models.

The integration of the data using an orthorhombic unit cell yielded a total of 20296 reflections to a maximum θ angle of 64.38° (0.85 Å resolution), of which 2726 were independent (average redundancy 7.445, completeness = 99.1%, R_{int} = 3.45%, R_{sig} = 2.06%) and 2575 (94.46%) were greater than $2\sigma(F^2)$. The final cell constants of $\underline{a}$ = 13.8088(2) Å, $\underline{b}$ = 8.54780(10) Å, $\underline{c}$ = 27.9659(4) Å, volume = 3300.95(8) Å^3, are based upon the refinement of the XYZ-centroids of reflections above 20 σ(I). The calculated minimum and maximum transmission coefficients (based on crystal size) are 0.8240 and 1.0000.

The structure was refined using the space group *Pbca*, with Z = 4 for the formula unit, $C_{30}H_{36}MnN_6O_2S_2$. The final anisotropic full-matrix least-squares refinement on F^2 with 203 variables converged at R1 = 4.79% [22], for the observed data and wR2 = 10.80% [23] for all data. The goodness-of-fit was 1.307. The largest peak in the final difference electron density synthesis was 0.358 $e^-/Å^3$ and the largest hole was -0.367 $e^-/Å^3$ with an RMS deviation of 0.066 $e^-/Å^3$. On the basis of the final model, the calculated density was 1.271 g/cm^3 and F(000), 1324 e^-.

CCDC 2404484 contains the supplementary crystallographic data for Mn(4,4'-DABPh)$_2$(NCS)$_2$(EtOH)$_2$ described in this paper. The data can be obtained free of charge from the Cambridge Crystallographic Data Centre *via www.ccdc.cam.ac.uk/data_request/cif.*

ACKNOWLEDGMENTS

The authors thank Eastern Illinois University for financial support through a Council on Faculty Research grant.

REFERENCES

1. J. Burmeister, *Coord. Chem. Rev.* **1990***, 105*, 77-133.
2. J. S. Wood, R. K. McMullan, *Acta Cryst.,* **1984**, *C40*, 1803-1806.
3. C. Wellm, T. Neumann, G. Gallo, A. M. Dziubyna, M. Rams, R. E. Dinnebier, C. Näther, *Cryst. Growth Des.,* **2020**, *20*, 3374-3385.
4. K. Mereiter, A. Preisinger, *Acta Cryst.,* **1988**, *C44*, 1178-1181.
5. C.-F. Wang, Z.-Y. Zhu, X.-G. Zhou, L.-H. Weng, Q.-S. Shen, Y.-G. Yan, *Inorg. Chem. Commun.,* **2006***, 9*, 1326-1330.
6. J.-U. Vogt, O. Haeckel, W. Preetz, *Z. Anorg. Allg. Chem.,* **1995***, 621,* 1033-1036.
7. J.-U. Rohde, W. Preetz, *Z. Anorg. Allg. Chem.,* **1998***, 624*, 1319-1323.
8. J.-U. Rohde, B. von Malottki, W. Preetz, *Z. Anorg. Allg. Chem.,* **2000**, *626*, 905-910.
9. J. Bandemehr, M. Conrad, F. Kraus, *Acta Cryst. E.,* **2017***, 73*, 1073-1075.
10. R. González, N. Barboza, R. Chiozzone, C. Kremer, D. Armentano, G. De Munno, J. Faus, *Inorg. Chim. Acta.,* **2008***, 361*, 2715-2720.
11. G. J. Palenik, G. R. Clark, *Inorg. Chem.,* **1970***, 9*, 2754-2760.
12. K. Nakamoto, *Infrared and Raman Spectra of Inorganic and Coordination Compounds: Part B: Applications in Coordination, Organometallic, and Bioinorganic Chemistry,* 6th ed., John Wiley & Sons, Inc.
13. A. Sabatini, I. Bertini, *Inorg. Chem.,* **1965***, 4*, 959-961.
14. Yu. V. Matveichuk, E. M. Rakhman'ko, and V. V. Yasinetskii, *Russ. J. Inorg. Chem.,* **2015***, 60*, 100-104.
15. C. Gh. Macarovici, R. Micu-Semeniuc, *Rev. Roum. Chim.,* **1971***, 16*, 1367-1376.
16. M. Kabesova, J. Gazo, *Chem. Papers,* **1980***, 34*, 800-841.
17. R. S. Rowland, Robin Taylor, *J. Phys. Chem.* **1996,** *100,* 7384-7391.
18. T. Steiner, *Angew. Chem. Int. Ed.* **2002***, 41*, 48-76.
19. L. Carlucci, G. Ciani, D. M. Proserpio, F. Porta, *CrystEngComm* **2006**, *8*, 696-706.
20. *APEX 3, v2017.3*; Bruker-AXS Inc.: Madison, WI, **2017**.
21. Sheldrick, G. M. *Acta Crystallogr., Sect. C: Struct. Chem.,* **2015**, *71*, 3−8.

22. $R_1 = \Sigma||F_o| - [\mathrm{F}_c||/\Sigma|F_o|$
23. $\mathrm{w}R_2 = \{\Sigma[\mathrm{w}(F_o^2 - \mathrm{F}_c^2)^2]/\Sigma[\mathrm{w}F_o^2]^2\}^{1/2}$